applied sciences

MDPI

*Article*

# Rapid Synthesis of Silver Nanowires in the Polyol Process with Conventional and Microwave Heating

**Grzegorz Dzido *, Aleksandra Smolska and Muhammad Omer Farooq**

Department of Chemical Engineering and Process Design, Silesian University of Technology, 44-100 Gliwice, Poland
* Correspondence: grzegorz.dzido@polsl.pl; Tel.: +48-322371913

**Abstract:** Silver nanowires (AgNWs) represent an excellent material for many advanced applications due to their thermal and electrical properties. However, synthesising materials with the desired characteristics requires knowledge of the parameters affecting their size and an appropriate fabrication method. This paper presents a study on the synthesis of silver nanowires using the polyol process by conventional and microwave heating. Various polyols (1,2-ethanediol, 1,3-propanediol, 1,3-butanediol, 1,4-butanediol, 1,5-pentanediol) with different viscosities and dielectric properties were used as reductants. It resulted in nanowires with an average diameter of 119–198 nm. It was found that, in contrast to the viscosity and dielectric constant of the alcohol used, the heating method had a limited effect on the average diameter and length value of the final product. The performed studies indicate an optimal strategy for fabricating one-dimensional silver nanostructures using the polyol method.

**Keywords:** batch synthesis; silver nanowires; polyol process; microwave-assisted synthesis

**Citation:** Dzido, G.; Farooq, M.O. Rapid Synthesis of Silver Nanowires in the Polyol Process with Conventional and Microwave Heating. *Appl. Sci.* **2023**, *13*, 4963. https://doi.org/10.3390/app13084963

Academic Editors: Andrey Kistanov and Elena Korznikova

Received: 23 February 2023
Revised: 2 April 2023
Accepted: 11 April 2023
Published: 14 April 2023



## 1. Introduction

Silver nanowires (AgNWs), defined as nanostructures with an average diameter of 10–200 nm and length of 5–100 μm [1], are intensively investigated regarding their application and fabrication methods. This results from their unique electrical [2], optical [3] and bactericidal properties [4], which are applied in optoelectronics [5] and advanced microelectronic solutions [6], as well as separation processes [7]. The fabrication of the structures under discussion is based on hard and soft templates [8] or methods of direct chemical synthesis [9]. Silver nanowires are, in most cases, synthesised in the so-called polyol process, in which multi-hydroxyl alcohol plays the roles of both solvent and reductant of the nanomaterial precursor [10]. Other authors have adapted and developed the polyol process to fabricate silver nanowires in heterogeneous [11] or homogeneous nucleation conditions [12]. In most cases, the reductant is 1,2-ethanediol, whereas the data pertinent to using other polyols are limited to 1,2-propanediol [13,14] or glycerol [15]. Because of their high values of loss tangent *tg(δ)* (Table S1—Supplementary Materials), polyols are characterised by an ability to absorb and transform microwave radiation into thermal energy. That is why they constitute an excellent environment for managing syntheses supported by microwave irradiation. One can notice a growing number of works related to the effective fabrication of AgNWs in processes in which dielectric heating is utilised [16].

The growth model of silver nanowires, reported in the open literature, results from the expansion of the {111} walls of five-fold-twinned decahedra seeds generated in the nucleation process [17]. The growth of opposite walls of twinned seeds leads to the creation of one-dimensional objects, such as nanowires or, more seldomly, V-shape nanorods [18]. Fabrication of the aforementioned seeds with the smallest possible sizes and preventing their lateral growth are believed to be the main factors determining the possibility of

obtaining long nanowires with thin diameters [19]. This is possible by tuning down the reduction kinetics and using an appropriate stabilising agent.

The anisotropic growth of the nanostructures under consideration is permitted by the use of polyvinylpyrrolidone (PVP) as a capping agent. Polyvinylpyrrolidone is adsorbed selectively on high surface energy planes of {100} due to an interaction between the oxygen from the PVP carboxyl group and silver. This effect promotes the extension of {111} walls with relatively lower surface energy [20].

The synthesis herein referred to is very often carried out with the presence of a mediating agent [21,22], which, with the silver ions occurring in the reaction environment, forms sparsely soluble compounds, e.g., chlorides [23], bromides [24], sulphides [20] and carbonates [25]. The addition of mediating agents provides electrostatic stabilisation of the newly formed nuclei. It reduces the concentration of free silver ions due to buffer formation that controls the rate of Ag(I) ions release and enhances oxidative digestion of the nuclei [13]. The synthesis can be intensified by conducting the polyol process in the presence of metal ions with various degrees of oxidation, e.g., Cu(I)/Cu(II) [26] or Fe(II)/Fe(III) [27]. As a result of the oxidation–reduction reactions taking place with metal ions, atomic oxygen adsorbed on the walls of nanostructures is scavenged. The presence of oxygen hinders the access of silver monomers to the expanded walls of nanostructures, particularly to the planes of {111}, whose expansion determines the growth of one-dimensional objects [22].

An effect of the viscosity of applied polyol on the shape, size and granulometric size distribution of the prepared nanoparticles is indicated in a few works [28,29]. Park noticed a decrease in the average size of synthesised silver nanoparticles concerning the increased viscosity of the reaction environment [30]. There are few references dealing with the effect of the viscosity of the reaction environment upon the properties of fabricated nanowires [31]. The viscosity is believed to affect the shape of obtained nanomaterials [32]. A synthesis occurring in a low-viscosity medium guarantees a sufficiently high diffusion rate of monomers supplied to the nanocrystal walls with both high and low surface energy. In the case of high-viscosity mediums, as a priority, monomers are added to high-energy facets to minimise the free surface energy.

Another factor influencing nanostructure nucleation and growth is the dielectric constant of the solvent used in the synthesis [33]. On the one hand, applying solvents with high dielectric constant values guarantees the stabilisation of the precursor ions and facilitates the digestion of fine nanoparticles already present in the solution [34]. On the other hand, in a solvent with a low dielectric constant, nanoparticle monomers are stabilised at high concentrations. A large number of monomers favours the formation of fine nanocrystals, which is crucial because of the growth of objects with high-aspect-ratio values [34,35].

Irrespective of viscosity, the reducing power of the applied polyol also influences the growth of nanoparticles. Any analysis of the latter effect is impeded [30], which is related to the problems inherent in separating the two said effects. Some information regarding the effect of the reducing power on the product size can be found in work on the synthesis of copper nanoparticles [36]. An analysis of the nucleation phenomena and the growth of nanoparticles led to a conclusion that large-sized objects should be expected for both high and low reduction rates of the precursor. It has also been ascertained that small water quantities may influence the output and growth rate of silver one-dimensional nanostructures [15].

A survey of the published reports on the polyol synthesis of AgNWs provides limited data on the impact of the viscosity and dielectric properties of the reaction environment on the final size of the nanostructures under consideration. To the best of our knowledge, there are no reports concerning the simultaneous impact of these parameters in the polyol synthesis of silver nanowires. Detailed studies have been carried out to address this deficiency using five polyols differing in viscosity, dielectric constant and structure. The syntheses were performed in batch mode, under conventional and microwave heating.

## 2. Materials and Methods

### *2.1. Chemicals*

Silver nanowires were synthesised using polyols with different molecular weights and lengths of aliphatic chains: 1,2-ethanediol p.a. (Chempur); 1,3-propanediol 99% (Alfa Aesar); 1,5-pentanediol, 97% (Alfa Aesar); 1,4-butanediol, +99% (Acros Organics); and 1,3-butanediol, 99% (Acros Organics). $AgNO_3$, p.a., (POCH), polyvinylpyrrolidone (PVP) K30 MW 40 kDa pure (Carl Roth GmbH) and $CuCl_2 \cdot 2H_2O$ p.a. (POCH) were used as a precursor, capping agent and mediating agent, respectively. All chemicals were used without additional purification. Figure S1 (Supplementary Materials) presents a graphical relationship between dynamic viscosity and temperature for each applied polyol. The data required for drawing the graphs were prepared using an Arrhenius-type equation from the commercially available software ChemCAD™:

$$\eta = \exp\left(A + \frac{B}{T} + C\ln(T)\right) \quad (1)$$

whereby *A*, *B* and *C* are individual constants dependent on the polyol used and *T*- temperature. It can be noticed that the viscosity of polyols depends on the molecular weight, length of the aliphatic chain and its structure. Table S1 (Supplementary Materials) shows the dielectric constant values for the applied multi-hydroxyl alcohols.

### *2.2. Methods*

Silver nanowires were synthesised in a bath process with conventional and dielectric heating. Experiments with conventional heating were carried out in a 250 $cm^3$ Erlenmeyer flask heated up on a magnetic stirrer (Heidolph MR, Schwabach, Germany) at a stirring intensity of 150 1/min. The microwave-assisted synthesis was performed in a laboratory installation shown in Figure 1, which is a modification of the previously used single-mode microwave system [28].

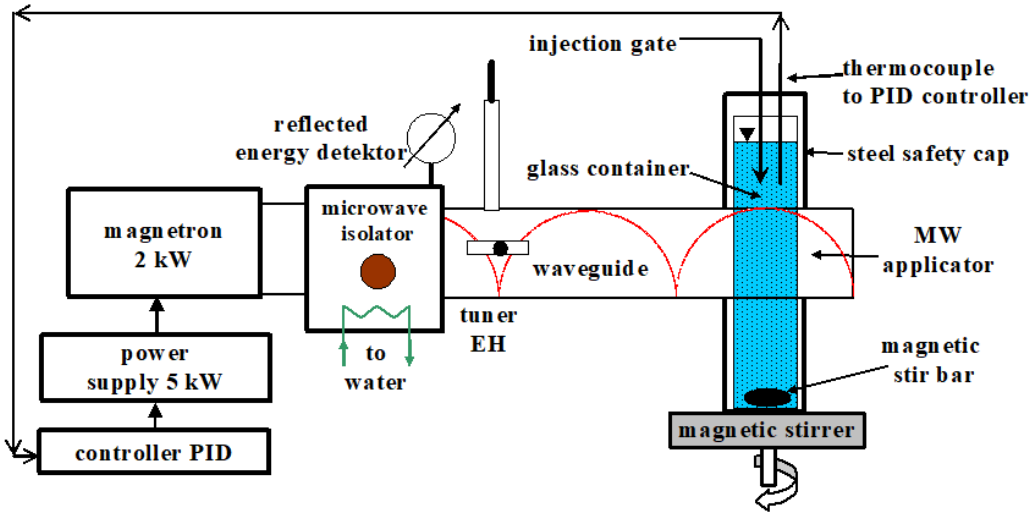


**Figure 1.** Single-mode laboratory setup for microwave-assisted synthesis of AgNWs.

In this setup, AgNWs were prepared inside a 30 mm ID glass cylinder placed inside a microwave applicator. The reaction mixture was mixed with a magnetic stirrer placed in the lower part of the cylinder. In both experimental setups, the temperature was controlled with an accuracy of ±0.5 °C. During a typical synthesis, 0.892 g of PVP was dissolved in 90 $cm^3$ of polyol, subjected to extensive mixing and its temperature was 80 °C. Then, 0.91 $cm^3$ of stock solution of 50 mM $CuCl_2$ was added and heated up to 170 °C. When the preset temperature had been reached, 0.910 g of $AgNO_3$ in 0.5 $cm^3$ of deionised

water was injected with a syringe into the reactor. Using a concentrated precursor solution guaranteed identical conditions for starting the nucleation and the growth of nanostructures in the course of syntheses. Following the addition of the precursor, the reaction mixture changed its colour to yellow, and with the progress of the reaction it became light grey and non-transparent. At the final stage of the process, the reaction mixture became grey with wispiness, which indicated the presence of one-dimensional nanostructures. After 5 min, the synthesis was completed by cooling the reactor in the water at room temperature. The final product was subjected to centrifugation at a rate of 20,000 1/min for 15 min. The supernatant was removed, and the remaining part was dispersed in DI water, centrifuged three times at 5000 1/min and stored in isopropanol for further characterisation.

### *2.3. Characterisation of Materials*

The morphology of fabricated materials was examined by an SEM microscope, TM 3000 (Hitachi, Tokyo, Japan), working at an accelerating voltage of 15 kV. A drop of the suspension was placed on a plate, dried at room temperature and then visualised. The diameter of AgNWs was determined using the image analysis software ImageJ. The average diameter and length of investigated structures were determined based on an analysis of 50 and 30 objects, respectively, with an aspect ratio greater than 10, observed in an SEM image. For HRTEM analysis of the product, a JEOL JEM 3010 field emission microscope working at an accelerating voltage of 300 kV was applied. The UV-Vis spectra of post-reaction mixture samples were recorded with a U-2800A spectrophotometer (Hitachi, Japan) in a quartz cuvette. Investigations into the crystalline phase were performed using X-ray diffractometry (XRD), with a X-Pert Pro device (Phillips, the Netherlands) and Cu K$\alpha$ radiation ($\lambda$ = 0.15418 nm). The results were analysed with the software Match! 3.1. Energy dispersive spectroscopy (EDS) analyses were carried out in a Phenom ProX SEM microscope (ThermoFisher Scientific, Waltham, MA, USA) to determine the atomic composition of selected samples of the synthesis product. The concentration of Ag(I) ions in the post-reaction solution was determined with an Eag/S-01 ion-selective electrode (Hydromet, Gdańsk, Poland). The total conversion $\alpha$ was calculated from the equation:

$$\alpha = \frac{c_i - c_f}{c_i} \cdot 100\% \quad (2)$$

where $c_i$, $c_f$ stand for, respectively, the initial and final Ag(I) concentrations.

## 3. Results and Discussion

Figure 2 presents typical XRD spectra for products manufactured with 1,3-propanediol and 1,3-butanediol as reductants in syntheses accompanied by conventional and dielectric heating.

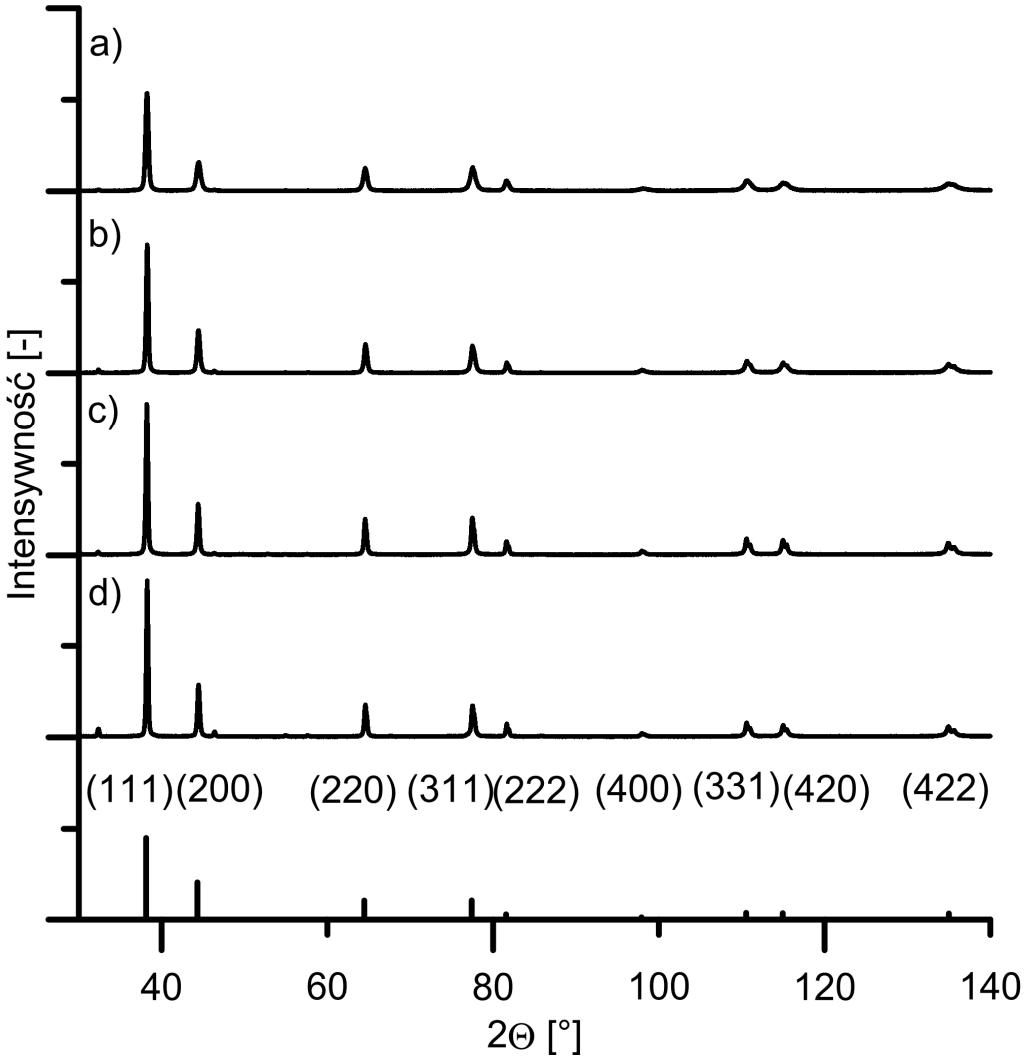


**Figure 2.** XRD patterns of the silver structures prepared in the conventional heating process, reductant (**a**) 1,3-butanediol or (**b**) 1,3-propanediol, and a microwave-assisted process, reductant (**c**) 1,3-butanediol or (**d**) 1,3-propanediol.

Diffraction peaks occurring for $2\Theta$ = 38.12, 44.31, 64.45, 77.41, 81.56, 97.90, 110.5 and 114.9° correspond with peaks which describe silver (ICSD sheet No. 01-071-6549). They correspond with crystallographic planes (111), (200), (220), (311), (222), (400), (331) and (420) of face-centred cubic Ag crystals. Low-intensity reflexes may be attributed to AgCl residues. A high-ratio value of intensities of reflexes (111) to (200) amounts, respectively, to 3.4 and 3.1 (Figure 2a,b) for conventional heating and 3.0 (Figure 2c,d) for microwave-assisted syntheses, so it exceeds the theoretical value of 2.2 (ICSD sheet No. 01-071-6549). It implies a considerable quantity of the {111} crystal planes in the samples examined and a preferential direction of growth of one-dimensional silver nanostructures [37]. The crystallite grain size was determined using the Williamson–Hall equation ($\beta\, cos(\Theta) = K\lambda/d_g + 4\varepsilon\, sin(\Theta)$) [38], whereby: $d_g$ is the average value of crystal grain size, $\lambda$ is the wavelength of the X-rays, $\beta$ is the total broadening of reflection due to crystallite size effect and lattice strain, $\Theta$ is the diffraction angle of a particular reflection, $\varepsilon$ is the lattice strain due to crystal imperfection and the K constant equals 0.90. After linearisation of the Williamson–Hall equation in the $\beta cos(\Theta)$ vs. $sin(\Theta)$ coordinates system (Figures 3 and 4), the average crystallite size and lattice strain were determined based on the knowledge of the intersection point of the straight and its slope found from the least squares method.

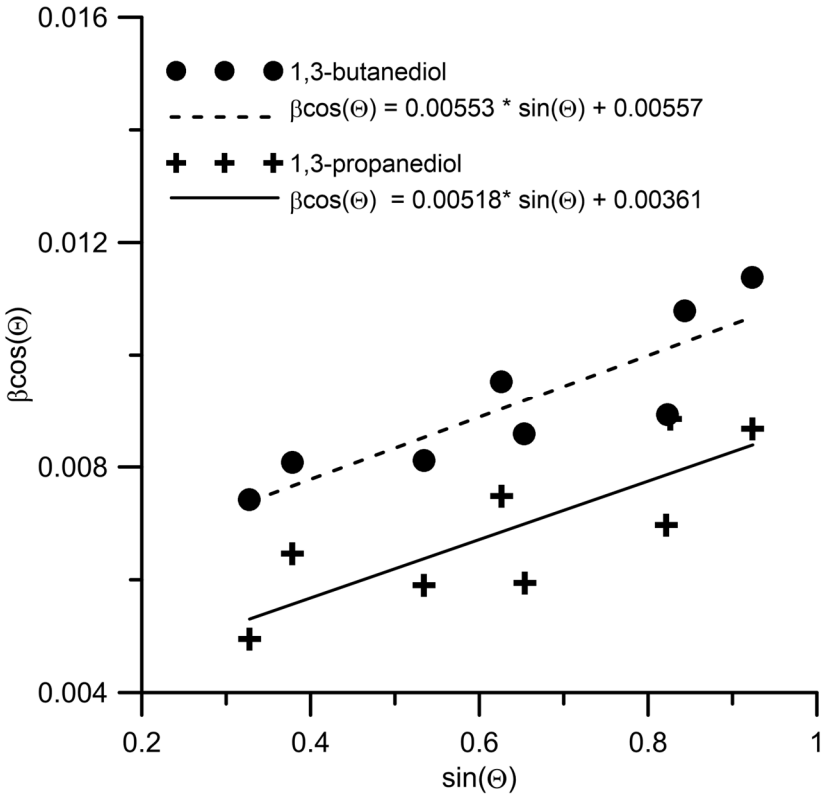


**Figure 3.** Williamson–Hall plot for AgNWs synthesised using different reductants under conventional heating conditions.

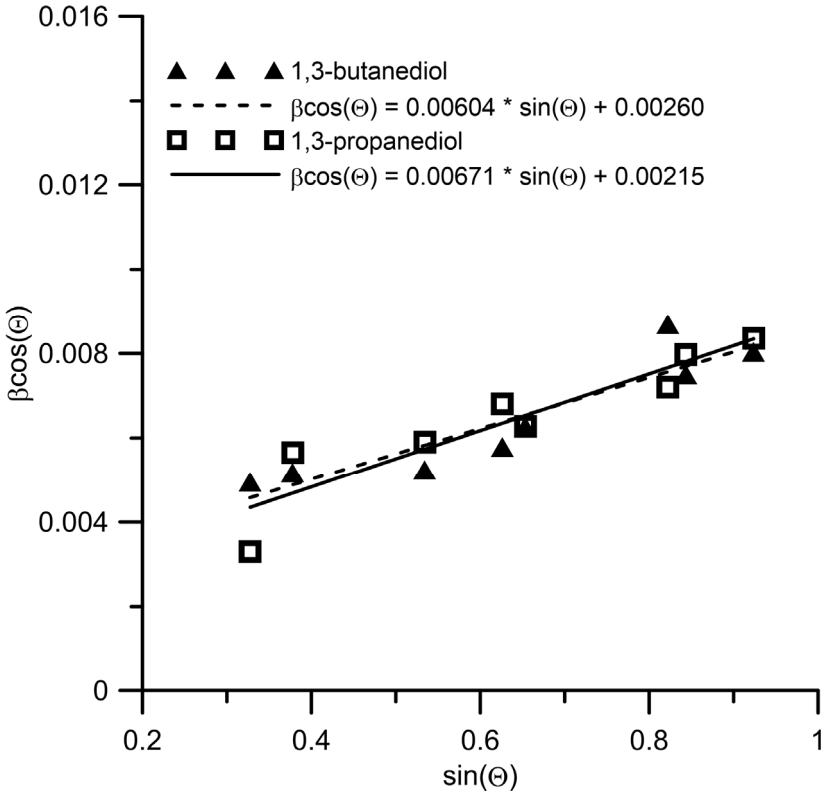


**Figure 4.** Williamson–Hall plot for AgNWs synthesised using different reductants in a microwave-assisted process.

The average crystallite sizes for silver nanowires synthesised in a batch process using 1,3-butanediol and 1,3-propanediol as reductants are 25 and 38 nm, respectively (Figure 3). The crystallite sizes shown above are smaller than those determined for the products synthesised using the same polyols in a microwave-assisted process. In the latter case, the crystallite sizes are 53 and 65 nm (Figure 4). In both analysed cases the results correspond with values obtained for silver nanoparticles [38,39]. The observed trend in crystallite size changes for both heating methods corresponds to that reported herein for average nanowire diameters. The experimentally determined lattice strains for all cases range from $1.3 \cdot 10^{-3}$ to $1.7 \cdot 10^{-3}$ and they are consistent with the values reported in the literature [39]. The lattice constant, defined according to the XRD diffraction pattern, amounts to 0.4086 nm and corresponds well with the value specified for silver (ICSD card No. 01-071-6549). Figure 5a presents a selected area electron diffraction (SAED) image recorded for silver nanowires obtained in the microwave-assisted process, in which 1,3-propanediol was used as a reducing agent. The SAED pattern contains more than two sets of diffraction spots that correspond with the multiply twinned crystal structures in the synthesis product. The EDS analysis for the same sample, shown in Figure 5b, proves that its main ingredient is silver. The EDS also contains a peak typical of chlorine presence whose source may be the mediating agent used in the synthesis.

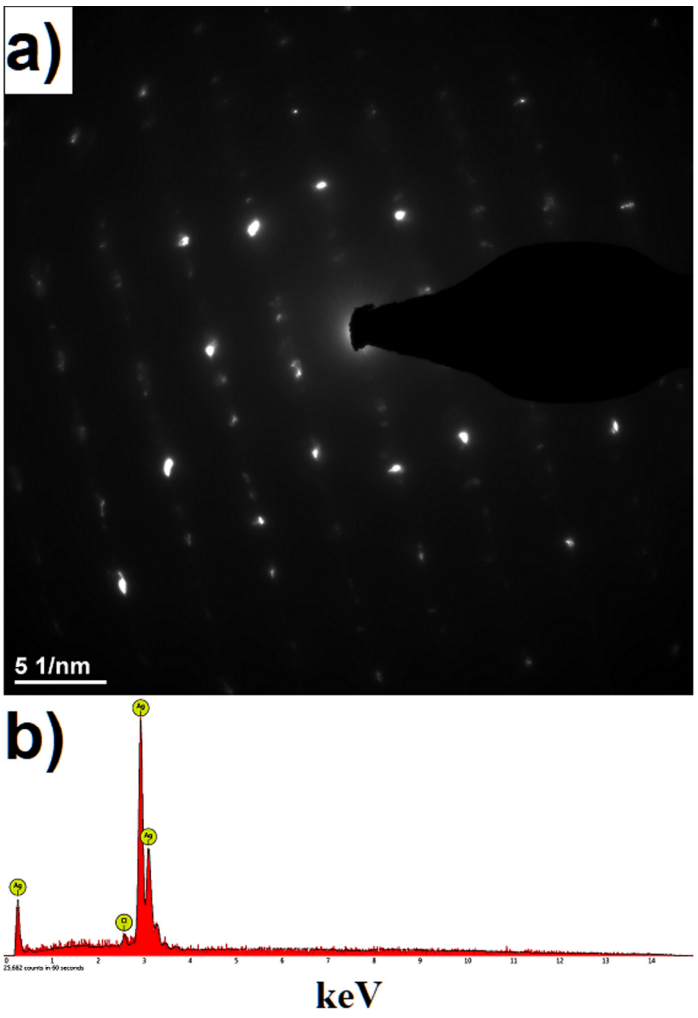


**Figure 5.** Silver nanowires synthesised in the microwave-assisted process, 1,3-propanediol reducer: (**a**) SAED pattern of AgNWs, (**b**) EDS spectrum for AgNWs.

Figures 6 and 7 portray SEM images, UV-Vis spectra, conversion coefficients, average diameter, length and the diameter distribution of the product synthesised with

conventional and dielectric heating. The presented results have been ordered in line with the increasing viscosity and decreasing dielectric constant value of polyols applied. Histograms of the product diameter distribution show the presence of a prominent fraction of nanowires with diameters between 40 and 200 nm and fractions of silver wires with diameters up to 320 nm. Nanowires with diameters above 100 nm are considered to have excellent mechanical stability at room temperature, which allows them to be easily machined to obtain a variety of electrically conductive circuits [40]. In addition, nanowires with diameters in this range are the preferred material for fabricating the active layer of a photovoltaic cell due to their effect on increasing optical haze. This effect increases light scattering and trapping inside the layer [41].

The observed lengths of the produced nanowires lie in the 2 to 26 µm range, while the average values for the analysed nanomaterial range from 3.3 to 10 µm. When comparing the corresponding values (Figures 6 and 7), no significant effect of the heating method on the average length can be observed. This leads to the conclusion that the determining factor for the length of the nanowires may lie in the capping agent used, i.e., polyvinylpyrrolidone. The influence of the molecular weight of PVP on the length of AgNWs has been noted by other authors [31].

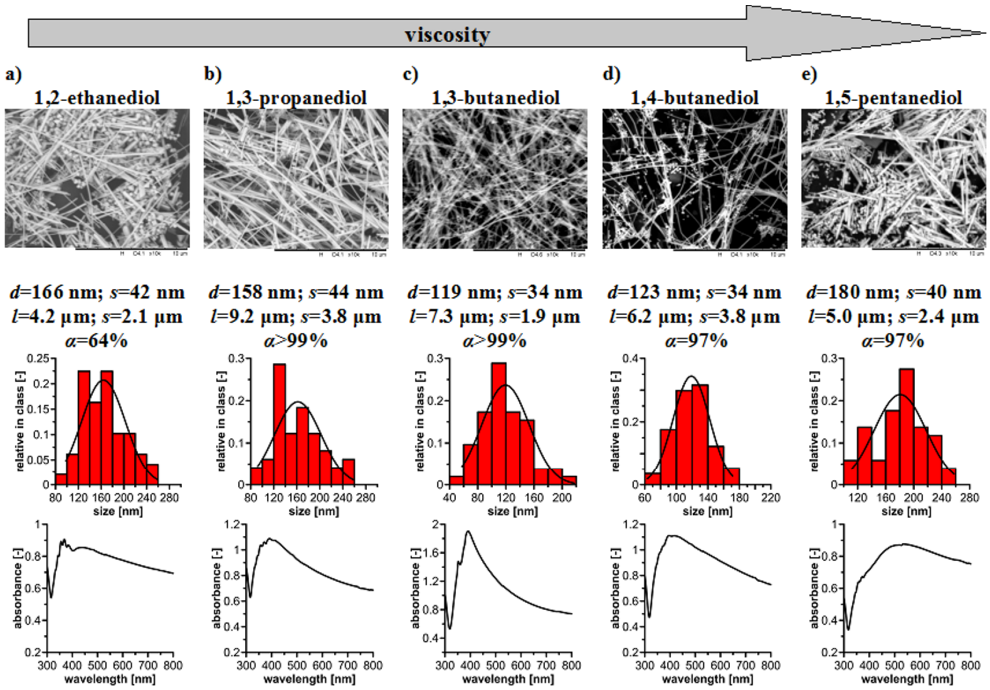


**Figure 6.** A summary of the properties of AgNWs produced in a batch process under conventional heating conditions: *d*, *l* = average diameter, length, respectively; s = standard deviation, *α* = conversion; scale bar 10 µm.

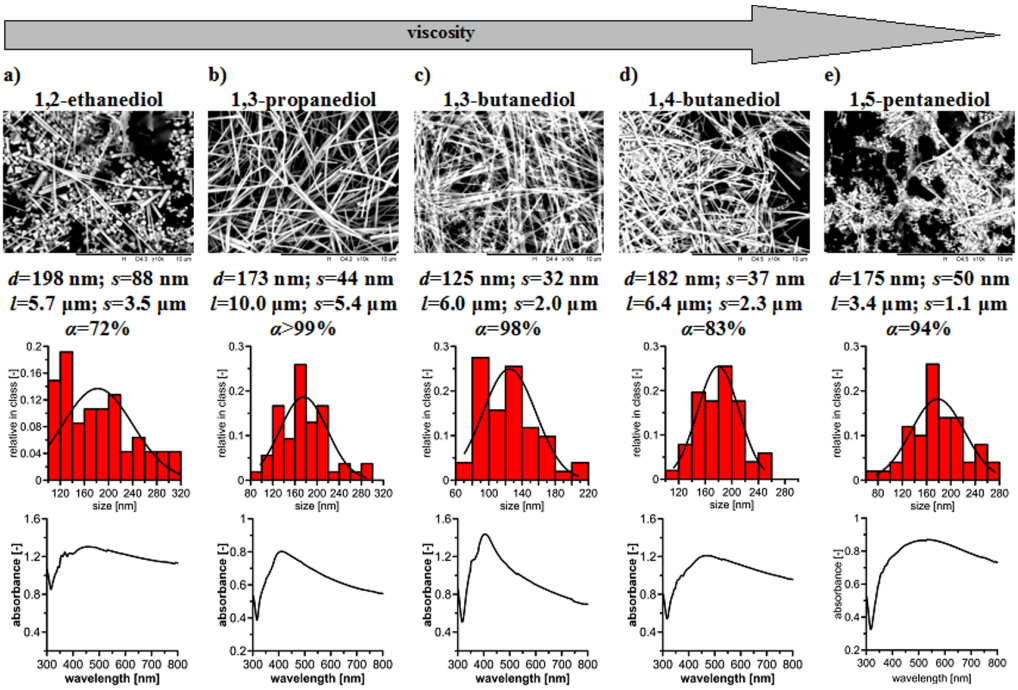


**Figure 7.** A summary of the properties of AgNWs produced in a batch, microwave-assisted process: *d*, *l* = average diameter, length, respectively; s = standard deviation; *α* = conversion; scale bar 10 µm.

As SEM images show, the morphology and average diameter of the final product considerably depends upon the type of polyol, which may be attributed to the simultaneous influence of viscosity and polarity of the solvent upon the nucleation process and the growth of nanowires. It is also worth noting that for the respective polyol, the final product has similar characteristics for the synthesis with conventional and dielectric heating. Significant differences in the diameter of the product prepared with 1,2-ethanediol and 1,3-propanediol, respectively equal to 166 and 158 nm, can be discerned while analysing the obtained results. In the latter case, the product is silver nanowires. In contrast, when 1,2-ethanediol is used, the product consists of structures with various shapes, confirmed by UV-Vis spectra with multiple maximums (Figures 6a and 7a). It is worth stressing that at the temperature at which the syntheses were carried out, the viscosity of the solvents is similar (Figure S1, Supplementary Materials). A plausible explanation for the differences observed in the final product characteristics may be some dissimilarities in the dielectric constant values of the polyols applied (Table S1, Supplementary Materials). It is believed that solvents having higher dielectric constant values can guarantee better stability of ions present in the solution [34]. This observation is corroborated by a rather low degree of conversion reached for both conventional (64%) and dielectric (72%) heating. It was also observed that in the case of syntheses conducted for 15 min (in this case, the results have not been shown), the conversion for both the heating methods exceeded 99%, and the morphology of the final products did not exhibit considerable differences.

On the other hand, using a solvent with a low dielectric constant value leads to forming a large number of nanoparticle monomers. This phenomenon accelerates the nucleation process and decreases the average size of the nuclei [42]. In the case under discussion, this causes a reduction in the average diameters of the product, which is corroborated by the results of synthesis with 1,3-propanediol (Figures 6b and 7b). Replacing the reductant with a polyol with a higher viscosity and a lower dielectric constant value (1,3-butanediol) led to further reduction in the diameter for both conventional and dielectric heating (Figures 6c and 7c). The tendency observed in the change in diameters confirms previous remarks on the effect of solvent polarity on the product size. In addition, an increase in viscosity hinders the diffusion-controlled transport of monomers. Consequently, the

formation of a larger quantity of smaller nuclei is promoted, which influences a diminution of the final product diameters [42]. The peaks visible in UV-Vis spectrograms (Figures 6c and 7c) for radiation wave lengths of 354 nm and 390–403 nm may be attributed to the plasmon response of metallic silver and transverse plasmon mode of nanowires [43–45].

The use of 1,4-butanediol is a good illustration of the effect of the dielectric constant value upon the average diameter of nanowires, which in this case is slightly higher than when 1,3-propanediol (Table S1, Supplementary Materials) is used. Despite a higher viscosity value which promotes a reduction in diameters, an increase in the product diameter is observed (Figures 6d and 7d). Lower conversion values for conventional and dielectric heating equal, respectively, 97 and 83% and can indicate a stabilisation of precursor ions.

As far as 1,5-pentanediol is concerned, despite its highest viscosity and lowest dielectric constant (Table S1, Supplementary Materials), nanowires are not the main product (Figures 6e and 7e). It may be caused by suppressing the growth of multiply twinned crystals in favour of single crystallite structures whose presence was observed by other authors in the synthesis using 1,5-pentanediol [29]. Many polyhedral objects and structures with a high aspect ratio value are observed in the case under analysis. The presence of objects with a low aspect ratio is confirmed by redshifted UV-Vis spectra (Figures 6e and 7e), whose peaks are recorded for the wavelength of 530 nm [43,46]. An obtuse-course spectrogram is observed for the 450–800 nm UV-Vis wavelength. The reason could be the presence of single crystallite nanoparticles for which the absorbance peaks lie precisely in the range of UV-Vis radiation [47]. Therefore, the observations of other authors are corroborated [32], according to which, in high-viscosity mediums the growth of higher-energy facets is privileged.

As far as conventional heating is concerned, when 1,2-ethanediol and 1,5-pentanediol are used in the synthesis, this leads to obtaining structures with the highest diameters compared to the product generated when other reductants are used. An analogical tendency was observed in microwave-assisted syntheses. It implies the complex effect of the above-discussed factors influencing the size of the fabricated nanowires and the possibility of obtaining a final product with an optimal diameter and composition. It is worth noticing that the occurrence of an optimum diameter was combined with the reduction rate of the precursor of copper nanoparticles [36]. At this investigation stage, correlating the reducing power of polyols used in syntheses to the average AgNW size is difficult. The reason is that it is hard to separate the effects of other factors, viz., viscosity or polarity of the solvent, which simultaneously influence the final product size and morphology. It should also be emphasised that the available literature lacks detailed data characterising the reactivity of multi-hydroxyl alcohols concerning synthesis in the polyol process.

In the case of syntheses carried out with 1,2-ethanediol, 1,3-propanediol, 1,3-butanediol and 1,4-butanediol used as reductants, one can observe a moderate effect exerted by the heating procedure applied upon the average product diameter. A comparison of the corresponding results obtained for conventional and dielectric heating shows that, in the latter case, the average diameters of silver nanowires produced are higher or almost equal, and the diameter distribution is shifted towards the fractions with higher diameter values. Except for 1,2-ethanediol, for the set of polyols under analysis, one can notice a slight effect of the heating procedure on the diameter standard deviation. These effects may be attributed to the diversified structures of test systems used for syntheses and the method of energy transfer. Dielectric heating provides uniform heating throughout the entire volume of the reaction medium, which promotes faster growth and a larger diameter of the nanowires produced.

In turn, despite stirring, the temperature distribution inside the conventionally heated reactor may not be uniform. Consequently, this diminishes the average growth rate of nanowires and influences their smaller size.

In Figure 8, one may see more V-shaped nanostructures sporadically occurring in the final product, formed during the reduction with 1,3-propanediol in the microwave-assisted process. The V-shaped structures consist of at least two nanowires or nanorods of

similar diameters. The angle between the respective units is obtuse or almost a straight angle, as seen in Figure 8a–d. It suggests that the growth of observed nanowires occurs by joining the ends of one-dimensional objects through the active planes {111}, which are then expanded using silver atoms that are the product of the reduction reaction or the dissolution of fine nanoparticles as a consequence of Ostwald ripening. A relatively small number of so-formed objects indicates that this mechanism is not predominant.

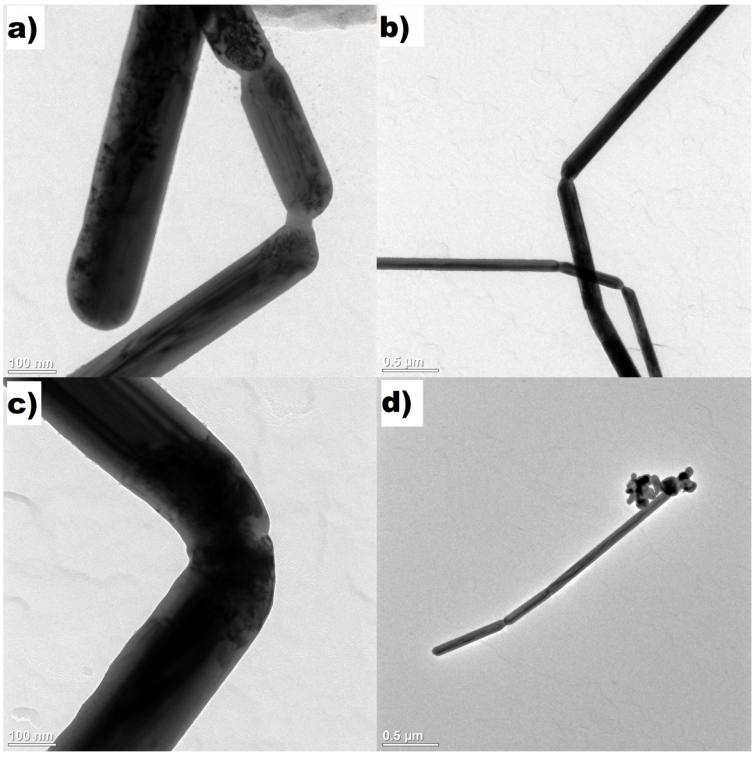


**Figure 8.** Growth of the AgNWs due to mutual attachments of one-dimensional objects: (**a**,**b**,**d**) different variants of nanowire-nanowire and nanowire-nanorod structures, (**c**) V-shape junction.

## 4. Conclusions

This article presents the experimental results of synthesising AgNWs with conventional and dielectric heating in the polyol process. The syntheses were carried out by applying polyols with different structures and properties. The effect of viscosity and the dielectric constant of the solvent used upon the morphology and average diameter of the final product was demonstrated, which permits optimisation of the final product parameters. It was observed that the heating procedure used for the laboratory system had a limited effect on the average diameter and length of the final product obtained. It was also ascertained that a different mechanism was responsible for the elongation of nanowires, which consists of the reciprocal addition of smaller 1D units and leads to forming V-shape structures. The obtained results can be used for planning the synthesis of AgNWs for application in advanced microelectronic appliances.

**Supplementary Materials:** The following supporting information [48-51] can be downloaded at: https://www.mdpi.com/article/10.3390/app13084963/s1, Figure S1: Temperature dependence of the viscosity of applied polyols; Table S1: Properties of applied polyols at 20 °C.

**Author Contributions:** Conceptualization, G.D., A.S. and M.O.F.; methodology, G.D., A.S. and M.O.F.; investigation, G.D., A.S. and M.O.F.; writing—original draft preparation, G.D. and A.S.; writing—review and editing, G.D., A.S. and M.O.F.; supervision, G.D. All authors have read and agreed to the published version of the manuscript.

**Funding:** This research received no external funding.

**Institutional Review Board Statement:** Not applicable.

**Informed Consent Statement:** Not applicable.

**Data Availability Statement:** In case any questions please send an email to corresponding author, grzegorz.dzido@polsl.pl.

**Acknowledgments:**. Publication supported by the Rector's pro-quality grant. The Silesian University of Technology, 04/030/RGJ22/0062.

**Conflicts of Interest:** The authors declare no conflict of interest.

## References

1. Heebo, H.; Amicucci, C.; Matteini, P.; Hwang, B. Mini review of synthesis strategies of silver nanowires and their applications. *Colloid Interface Sci. Commun.* **2022**, *50*, 100663. https://doi.org/10.1016/j.colcom.2022.100663.
2. Li, R.; Peng, Q.; Han, B.; Ke, Y.; Wang, X.; Lu, X.; Wu, X.; Kong, J.; Ren, Z.; Akinoglu, E.M.; et al. Plasmonic refraction-induced ultrahigh transparency of highly conducting metallic networks. *Laser Photonics Rev.* **2016**, *10*, 465–472. https://doi.org/10.1002/lpor.201500271.
3. Yang, X.; Bao, D.; Li, B. Light transfer from quantum-dot-doped polymer nanowires to silver nanowires. *RSC Adv.* **2015**, *5*, 60770–60774. https://doi.org/10.1039/c5ra11566c.
4. Valodkar, M.; Sharma, P.; Kanchan, D.K.; Thakore, S. Conducting and antimicrobial properties of silver nanowire-waxy starch nanocomposites. *Int. J. Green Nanotechnol. Phys. Chem.* **2010**, *2*, 10–19. https://doi.org/10.1080/19430876.2010.488209.
5. Li, J.; Qi, S.; Li, J.; Zhanga, M.; Wang, Z. A highly thermostable and transparent lateral heat spreader based on silver nanowire/polyimide composite. *RSC Adv.* **2015**, *5*, 59398–59402. https://doi.org/10.1039/c5ra08900j.
6. Langley, D.; Giusti, G.; Mayousse, C.; Celle, C.; Bellet, D.; Simonato, J.P. Flexible transparent conductive materials based on silver nanowire networks: A review. *Nanotechnology* **2013**, *24*, 452001. https://doi.org/10.1088/0957-4484/24/45/452001.
7. Liu, X.; He, L.; Zheng, J.; Guo, J.; Bi, F.; Ma, X.; Zhao, K.; Liu, Y.; Song, R.; Tang, Z. Solar-light-driven renewable butanol separation by core–shell Ag@ZIF-8 nanowires. *Adv. Mater.* **2015**, *27*, 3273–3277. https://doi.org/10.1002/adma.201405583.
8. Sun, Y. Silver nanowires—Unique templates for functional nanostructures. *Nanoscale* **2010**, *2*, 1626–1642. https://doi.org/10.1039/c0nr00258e.
9. Sun, Y.; Xia, Y. Large-scale synthesis of uniform silver nanowires through a soft; self-seeding polyol process. *Adv. Mater.* **2002**, *14*, 833–837. https://doi.org/10.1002/1521-4095.
10. Fivet, F.; Brayner, R. The polyol process. In *Nanomaterials: A Danger or a Promise*; Brayner, R., Fievet, F., Coradin, T., Eds.; Springer: London, UK, 2013; pp. 1–25.
11. Tsuji, M.; Matsumoto, K.; Jiang, P.; Matsuo, R.; Tang, X.L.; Kamarudin, K.S.N. Roles of Pt seeds and chloride anions in the preparation of silver nanorods and nanowires by microwave-polyol method. *Colloids Surf. A Physicochem. Eng. Asp.* **2008**, *316*, 266–277. https://doi.org/10.1016/j.colsurfa.2007.09.014.
12. Chen, C.; Wang, L.; Jiang, G.; Yang, Q.; Wang, J.; Yu, H.; Chen, T.; Wang, C.; Chen, X. The influence of seeding conditions and shielding gas atmosphere on the synthesis of silver nanowires through the polyol process. *Nanotechnology* **2006**, *17*, 466–474. https://doi.org/10.1088/0957-4484/17/2/021.
13. Johan, M.R.; Aznan, N.A.K.; Yee, S.T.; Ho, I.H.; Ooi, S.W.; Singho, N.D.; Aplop, F. Synthesis and growth mechanism of silver nanowires through different mediated agents ($CuCl_2$ and NaCl) polyol process. *J. Nanomater.* **2014**, *2014*, 105454. https://doi.org/10.1155/2014/105454.
14. Sim, H.; Kim, Ch.; Bok, S.; Kim, M.K.; Oh, H.; Lim, G.H.; Cho, S.M.; Lim, B. Five-minute synthesis of silver nanowires and their roll-to-roll processing for large-area organic light emitting diodes. *Nanoscale* **2018**, *10*, 12087–12092. https://doi.org/10.1039/c8nr02242a.
15. Yang, C.; Gu, H.; Lin, W.; Yuen, M.M.; Wong, C.P.; Xiong, M.; Gao, B. Silver nanowires: From scalable synthesis to recyclable foldable electronics. *Adv. Mater.* **2011**, *23*, 3052–3056. https://doi.org/10.1002/adma.201100530.
16. Nghia, N.V.; Truong, N.N.K.; Thong, N.M.; Hung, N.P. Synthesis of nanowire—Shaped silver by polyol process of sodium chloride. *Int. J. Mater. Chem.* **2012**, *2*, 75–78. https://doi.org/10.5923/j.ijmc.20120202.06.
17. Wiley, B.; Sun, Y.; Xia, Y. Synthesis of silver nanostructures with controlled shapes and properties. *Acc. Chem. Res.* **2007**, *40*, 1067–1076. https://doi.org/10.1021/ar7000974.
18. Liu, X.; Zhang, F.; Huang, R.; Pan, C.; Zhu, J. Capping modes in PVP-directed silver nanocrystal growth: Multi-twinned nanorods versus single-crystalline nano-hexapods. *Cryst. Growth. Des.* **2008**, *8*, 1916–1923.
19. da Silva, R.R.; Yang, M.; Choi, S.I.; Chi, M.; Luo, M.; Zhang, C.; Li, Z.Y.; Camargo, P.H.C.; Ribeiro, S.J.L.; Xia, Y. Facile synthesis of sub-20 nm silver nanowires through a bromide-mediated polyol method. *ACS Nano* **2016**, *10*, 7892–7900. https://doi.org/10.1021/acsnano.6b03806.
20. Chen, D.; Qiao, X.; Qiu, X.; Chen, J.; Jiang, R. Convenient, rapid synthesis of silver nanocubes and nanowires via a microwave-assisted polyol method. *Nanotechnology* **2010**, *21*, 025607. https://doi.org/10.1088/0957-4484/21/2/025607.
21. Nandikonda, S.; Davis, E.W. Parameters affecting the microwave-assisted polyol synthesis of silver nanorods. *ISRN Nanotechnol.* **2011**, *2011*, 104086. https://doi.org/10.5402/2011/104086.

22. Wiley, B.; Sun, Y.; Xia, Y. Polyol synthesis of silver nanostructures: Control of product morphology with Fe(II) or Fe(III) species. *Langmuir* **2005**, *21*, 8078–8080. https://doi.org/10.1021/la050887i.
23. Chou, K.S.; Hsua, C.Y.; Liu, B.T. Salt-mediated polyol synthesis of silver nanowires in a continuous-flow tubular reactor. *RSC Adv.* **2015**, *5*, 29872–29877. https://doi.org/10.1039/c5ra00320b.
24. Chen, C.; Wang, L.; Jiang, G.; Zhou, J.; Chen, X.; Yu, H.; Yang, Q. Study on the synthesis of silver nanowires with adjustable diameters through the polyol process. *Nanotechnology* **2006**, *17*, 3933–3938. https://doi.org/10.1088/0957-4484/17/15/054.
25. Liu, S.; Sun, B.; Li, J.G.; Chen, J. Silver nanowires with rounded ends: Ammonium carbonate-mediated polyol synthesis; shape evolution and growth mechanism. *CrystEngComm* **2014**, *16*, 244–251. https://do.org/10.1021/cg701128b.
26. Amirjani, A.; Marashi, P.; Fatmehsari, D.H. Effect of $AgNO_3$ addition rate on aspect ratio of $CuCl_2$–mediated synthesized silver nanowires using response surface methodology. *Colloids Surf. A Physicochem. Eng. Asp.* **2014**, *444*, 33–39. https://doi.org/10.1016/j.colsurfa.2013.12.033.
27. Jiu, J.; Araki, T.; Wang, J.; Nogi, M.; Sugahara, T.; Naga, S.; Koga, H.; Suganum, K.; Nakazawa, E.; Hara, M.; et al. Facile synthesis of very-long silver nanowires for transparent electrodes. *J. Mater. Chem. A* **2014**, *2*, 6326–6330. https://doi.org/10.1039/c4ta00502c.
28. Dzido, G.; Markowski, P.; Małachowska-Jutsz, A.; Prusik, K.; Jarzębski, A.B. Rapid continuous microwave-assisted synthesis of silver nanoparticles to achieve very high productivity and full yield: From mechanistic study to optimal fabrication strategy. *J. Nanoparticle Res.* **2015**, *17*, 27. https://doi.org/10.1007/s11051-014-2843-y.
29. Tao, A.R.; Habas, S.; Yang, P. Shape control of colloidal metal nanocrystals. *Small* **2008**, *4*, 310–325.
30. Park, K.H.; Im, S.H.; Park, O.O. The size control of silver nanocrystals with different polyols and its application to low-reflection coating materials. *Nanotechnology* **2011**, *22*, 045602. https://doi.org/10.1088/0957-4484/22/4/045602.
31. Zhao, W.; Wang, S.S.; Cao, H.T.; Xie, L.H.; Hong, C.S.; Jin, L.Z.; Yu, M.N.; Zhang, H.; Zhang, Z.Y.; Huang, L.H.; et al. An eco-friendly water-assisted polyol method to enhance the aspect ratio of silver nanowires. *RSC Adv.* **2019**, *9*, 1933–1938. https://doi.org/10.1039/c8ra08810a.
32. Yang, T.; Han, Y.; Li, J. Manipulating silver dendritic structures via diffusion and reaction. *Chem. Eng. Sci.* **2015**, *138*, 457–464. https://doi.org/10.1016/j.ces.2015.08.017.
33. Zhao, X.B.; Ji, X.H.; Zhang, Y.H.; Lu, B.H. Effect of solvent on the microstructures of nanostructured $Bi_2Te_3$ prepared by solvothermal synthesis. *J. Alloys Compd.* **2004**, *368*, 349–352. https://doi.org/10.1016/j.jallcom.2003.08.070.
34. Qingqing, W.; Gang, X.; Gaorong, H. Solvothermal synthesis and characterization of uniform CdS nanowires in high yield. *J. Solid State Chem.* **2005**, *178*, 2680–2685. https://doi.org/10.1016/j.jssc.2005.06.005.
35. Wei, X.; Xu, G.; Ren, Z.; Wang, Y.; Shen, G.; Han, G. Synthesis of highly dispersed barium titanate nanoparticles by a novel solvothermal method. In *Progress in Nanotechnology Processing*; Wiley: Hoboken, NJ, USA, 2010; pp. 33–36.
36. Blosi, M.; Albonetti, S.; Dondi, M.; Martelli, C.; Baldi, G. Microwave-assisted polyol synthesis of Cu nanoparticles. *J. Nanoparticle Res.* **2011**, *13*, 127–138. https://doi.org/10.1007/s11051-010-0010-7.
37. Gomez-Acosta, A.; Manzano-Ramirez, A.; Lopez-Naranjo, E.J.; Apatiga, L.M.; Herrera-Basurto, R.; Rivera-Munoz, E.M. Silver nanostructure dependence on the stirring-time in a high-yield polyol synthesis using a short-chain PVP. *Mater. Lett.* **2015**, *138*, 167–170. https://doi.org/10.1016/j.matlet.2014.09.109.
38. Sundeep, D.; Kumar, D.V.; Subba Rao, P.S.; Ravikumar, R.V.S.S.N.; Gopala Krishna, A. Green synthesis and characterization of Ag nanoparticles from *Mangifera indica* leaves for dental restoration and antibacterial applications. *Prog. Biomater.* **2017**, *6*, 57–66. https://doi.org/10.1007/s40204-017-0067-9.
39. Biju, V.; Sugathan, N.; Vrinda, V.; Salini, L. Estimation of lattice strain in nanocrystalline silver from X-ray diffraction line broadening. *J. Mater. Sci.* **2008**, *43*, 1175–1179. https://doi.org/10.1007/s10853-007-2300-8.
40. Jiang, P.; Li, S.Y.; Xie, S.S.; Gao, Y.; Song, L. Machinable long PVP-stabilized silver nanowires. *Chem. Eur. J.* **2004**, *10*, 4817–4821. https://doi.org/10.1002/chem.200400318.
41. Andrés, L.J.; Menéndez, M.F.; Gómez, D.; Martínez, A.L.; Bristow, N.; Kettle, J.P.; Menéndez, A.; Ruiz, B. Rapid synthesis of ultra-long silver nanowires for tailor-made transparent conductive electrodes: Proof of concept in organic solar cells. *Nanotechnology* **2015**, *26*, 265201. https://doi.org/10.1088/0957-4484/26/26/265201.
42. Yu, J.C.; Zhang, L.; Li, Q.; Kwong, K.W.; Xu, A.W.; Lin, J. Sonochemical preparation of nanoporous composites of titanium oxide and size-tunable strontium titanate crystals. *Langmuir* **2003**, *19*, 7673–7675. https://doi.org/10.1021/la0345035.
43. Sun, Y.; Yin, Y.; Mayers, B.T.; Herricks, T.; Xia, Y. Uniform silver nanowires synthesis by reducing $AgNO_3$ with ethylene glycol in the presence of seeds and poly(vinyl pyrrolidone). *Chem. Mater.* **2002**, *14*, 4736–4745. https://doi.org/10.1021/cm020587b.
44. Zhang, W.; Chen, P.; Gao, Q.; Zhang, Y.; Tang, Y. High-concentration preparation of silver nanowires: Restraining in situ nitric acidic etching by steel-assisted polyol method. *Chem. Mater.* **2008**, *20*, 1699–1704. https://doi.org/10.1021/cm7022554.
45. Zhu, J.J.; Kan, C.X.; Wan, J.G.; Han, M.; Wang, G.H. High-yield synthesis of uniform Ag nanowires with high aspect ratios by introducing the long-chain PVP in an improved polyol process. *J. Nanomater.* **2011**, *2011*, 982547. https://doi.org/10.1155/2011/982547.
46. Kan, C.X.; Zhu, J.J.; Zhu, X.G. Silver nanostructures with well-controlled shapes: Synthesis; characterization and growth mechanisms. *J. Phys. D Appl. Phys.* **2008**, *41*, 155304. https://doi.org/10.1002/anie.200400655.
47. Tao, A.; Sinsermsuksakul, P.; Yang, P. Polyhedral silver nanocrystals with distinct scattering signatures. *Angew. Chem. Int. Ed.* **2006**, *45*, 4597–4601. https://doi.org/10.1002/smll.200701295.
48. Kappe, C.O. Controlled microwave heating in modern organic synthesis. *Angew. Chem. Int. Ed.* **2004**, *43*, 6250–6284.

49. Gabriel, C.; Gabriel, S.; Grant, E.H.; Halstead, B.S.J.; Mingos, D.M.P. Dielectric parameters relevant to microwave dielectric heating. *Chem. Sci. Rev.* **1998**, *27*, 213–223. https://doi.org/10.1039/A827213Z.
50. Sudo, S.; Shinyashiki, N.; Kitsuki, Y.; Yagihara, S. Dielectric relaxation time and relaxation time distribution of alcohol-water mixtures. *J. Phys. Chem. A* **2002**, *106*, 458–464. https://doi.org/10.1021/jp013117y.
51. Wohlfarth, C. Permittivity (dielectric constant) of liquids; In *Handbook of Chemistry and Physics*, 93rd ed.; Haynes, W.M. Ed.; CRC Press: Boca Raton, UK, 2016; Volume 6; pp. 135–175.